Transmission over SSMF at 850 nm: bimodal propagation and equalization

Pau Medina, Vicenç Almenar, and Juan Luis Corral, Senior Member, IEEE

***Abstract*—The combination of 850 nm vertical-cavity surface-emitting laser (VCSEL) with standard single-mode fiber (SSMF) presents an effective and low-cost interface to increase the reach provided by multi-mode fiber (MMF) links. At 850 nm, SSMF propagates two modes and in this work it has been experimentally shown that the different commercially available SSMF's present dissimilar values of differential mode delay (DMD). To cope with this unequal behavior of modal dispersion, we propose a scheme based on bidirectional decision feedback equalization (BiDFE) to overcome limited performance of other solutions as mode filtering or classical equalizers. A single span SSMF cabling model, including a measurement-derived statistical characterization of optical connectors, is simulated to evaluate the reach provided by the equalizer attending to both the conditions of the fiber excitation and the characteristics of the VCSEL. A minimum 1.45 km link length at 10 Gb/s is achieved if a Linear Combining BiDFE (LC-BiDFE) equalizer is included in the receiver, whatever laser launching condition and employing a single-transverse mode VCSEL. If a multi-transverse mode VCSEL is used, the reach provided by LC-BiDFE is slightly reduced but assuring a minimum coverage of 1.15 km.**

***Index Terms*—Channel model, decision feedback equalizers, modal dispersion, mode coupling, numerical simulation, optical connectors, optical fiber communication, single-mode fiber, vertical cavity surface emitting laser.**

I. Introduction

THE availability of energy-efficient and cost-effective vertical-cavity surface-emitting lasers (VCSEL's) at 850 nm combined with optimized designs of multimode fiber (MMF) have been stablished as a low-cost solution for short range high-speed optical data links. For example, the 10GBASE-SR interface, included in the 10 Gigabit Ethernet (10GbE) standard and operating over MMF, defines a maximum reach of 300 m with a bit error rate (BER) below 10^{-12} using laser-optimized 50 µm fiber (OM3) combined with 850 nm VCSEL's. By using a new class of standardized MMF fiber (OM4), the coverage could be extended up to 400 m [1]. Great efforts have been carried out in order to increase the effective modal bandwidth of MMF, which has also resulted in an increase in the cost of new fiber deployments; besides, the redeployment of these new MMF types prevents reusing of legacy links.

The use of 850 nm VCSEL's for transmission over SSMF constitutes a promising low-cost solution to improve the link reach provided by MMF. At 850 nm, only 2 modes propagate in SSMF causing inter-symbol interference (ISI) due to differential mode delay (DMD). SMF standardization by regulators like ANSI/TIA/EIC and ITU have defined specifications of the fiber in the region between 1260 and 1625 nm [2]. The lack of specifications for SSMF at the 850 nm window causes bimodal propagation characteristics to differ between different models and manufacturers.

A mode filter (MF) to reject the higher mode and reduce accordingly the ISI has been reported in [3] giving a reach of 1 km with a BER below 10^{-12} at 10 Gb/s. The main problems of using MF are twofold: each MF reduces the transmitted signal power when the higher mode is rejected, and a MF must be included before each splice or connector, where coupling between both modes can be induced. Thus, depending on the VCSEL launch conditions or the connectors misalignment, the link reach could be seriously reduced.

Another approach to cancel the ISI caused by the DMD is the employment of an equalizer. The Maximum Likelihood Sequence Estimator (MLSE) is the optimum receiver from the point of view of minimizing the error probability, but its complexity is exponential with the channel memory (maximum channel delay in symbol period units). As a consequence, for practical implementations a suboptimal approach is preferred. For example, the use of decision feedback equalization (DFE) in optical communications has been extensively analyzed in the literature [4] and has been recently standardized for 10GbE optical link solutions on MMF. For instance, 10GBASE-LRM includes an electronic dispersion compensation chip that enables the equalization of incoming modal dispersion to achieve error-free transmission over 220 m links of any MMF type at 1310 nm, including Fiber Distributed Data Interface (FDDI)-grade and OM1 fibers [1]. Following this approach, in this paper, we propose the use of an evolved equalizer scheme based on the classical DFE implementation to deal with the bimodal propagation over SSMF at 850 nm whatever fiber model is used; this advanced equalization scheme is called in the literature Bidirectional DFE (BiDFE) [5], [6].

Several examples of commercially available SSMF have

P. Medina and V. Almenar are with Instituto de Telecomunicaciones y Aplicaciones Multimedia, Universitat Politècnica de València, Valencia 46022, Spain (e-mail: pamese@teleco.upv.es; valmenar@dcom.upv.es).

J. L. Corral is with Nanophotonics Technology Center, Universitat Politècnica de València, Valencia 46022, Spain (e-mail: jlcorral@ntc.upv.es).

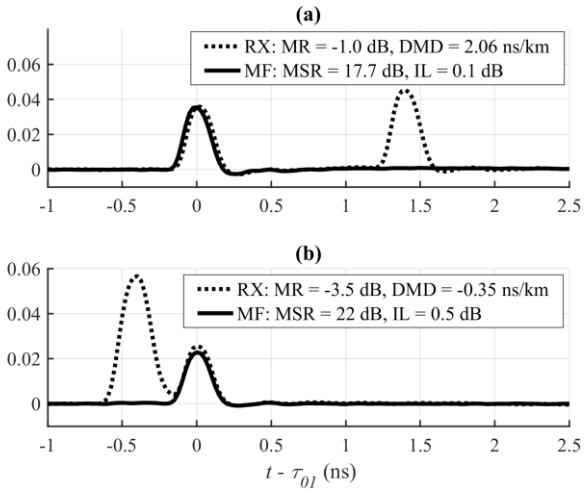

Fig. 1. Single pulse propagation through 680 m Corning SMF-28 (a), and 1153 m Draka ESSMF (b). Signals corresponding to received (RX), and mode filtered received (MF).

been experimentally characterized and their main parameters are presented in section II. Also in section II, the effect of mode coupling, induced by optical connectors, is studied, by means of measurements and numerical simulations, to evaluate its impact on SSMF link performance. The equalizer configurations able to cope with the ISI caused by the bimodal propagation are presented in section III. In section IV, the reach improvement provided by the proposed equalizers are assessed by considering a complete model of the SSMF link including the limiting factors of SSMF propagation and modal coupling, and the effects of using a VCSEL as optical source. Finally, in section V the main conclusions are derived.

II. Bimodal propagation over SSMF at 850 nm

In this section, the main features of SSMF affecting the signal transmission at 850 nm are studied: modal dispersion and mode coupling. To evaluate modal dispersion, several commercially available models of SSMF have been measured to check the variability of DMD values between them. In order to characterize the mode coupling caused by misaligned optical connectors, the magnitude of this misalignment has been derived from mode coupling measurements when the connectors are excited just by the fundamental mode, and this result have been extended to all other mode-coupling cases. The measures have been performed in a setup composed by a directly modulated VCSEL (Finisar HFE6x92-x61 model) and its corresponding photodiode (HFD6380-418); the electrical photo-detected signals were captured by a Keysight Infiniium oscilloscope at 40 GSa/s and their samples were digitally filtered by a 4th order Bessel filter with a 7.5 GHz cut-off frequency.

A. Modal Dispersion: Differential Mode Delay (DMD)

At 850 nm, SSMF propagates two linear polarized modes, LP_{01} and LP_{11}, each one at a different group velocity. The difference between the delays of both modes per unit length defines DMD. Each mode also suffers from group velocity dispersion (GVD): although its values for both modes at 850 nm are higher (around ~85 ps/(km·nm) [7]) than those corresponding to typical single-mode operation wavelengths (16 ps/(km·nm) at 1550 nm and close to zero at 1310 nm), its effect in pulse broadening is much lower than modal dispersion. Nevertheless GVD is not negligible and, attending to the spectral width of an optical source like a VCSEL, its influence in link performance could be significant as we will show in section IV.

In the literature, there exist several studies about the bimodal propagation over SSMF at 850 nm that show the divergence in the measured DMD values. They range from 1.2 ns/km [8], [9] to 2.5 ns/km [10] or even 3.3 ns/km [11]; however, the most usual results correspond to DMD values between 2.1 and 2.3 ns/km [3], [12]-[15]. Moreover, a specially designed fiber, compliant with SMF standards [2] but optimized for 850 nm, was shown to achieve DMD values below 0.1 ns/km [7], [16].

The first measured fiber was the SMF-28 from Corning, one of the most deployed SSMF models. Fig. 1a shows the detected signals corresponding to a transmitted single pulse of 0.23 ns width (full width at half maximum) received after a 680 m span of fiber without MF, and with a MF made by coiling the end-tail of the fiber span in order to filter out the LP_{11} mode contribution. A DMD of 2.1 ns/km was measured, here defined as the difference between the delays of LP_{11} and LP_{01} modes per unit length: $DMD = (\tau_{11} - \tau_{01})/L_{TX}$. Modal ratio is defined as the optical power ratio between both modes, $MR = P_{01}/P_{11}$, and the measurements shown in Fig. 1a correspond to a fiber launching condition that excites slightly more LP_{11} mode than LP_{01} (MR = –1 dB).

The second measured fiber was the Enhanced SSMF (ESSMF) by Draka, which is also compliant with [2], that allows high bit rate transmissions across the entire 1260 to 1625 nm bandwidth. Fig. 1b shows the same detected pulses as before in a fiber span of 1153 m. The main difference with SMF-28 is a DMD = –0.35 ns/km, where the negative sign means that fundamental mode travels along the fiber slower than the LP_{11} mode, similar as it was reported in [7], [16]. Here again, the VCSEL excites a stronger LP_{11} mode: MR = –3.5 dB.

Finally, measures of a single pulse propagated over a link of SMF-28e fiber, which is offered by Corning as an evolved version of SMF-28, but offering enhanced capabilities and specifications while providing full compatibility with legacy SMF, presented a DMD value of 2.3 ns/km.

B. Fiber misalignment: mode coupling and loss

Various physical mechanisms can lead to coupling between propagated modes. We can roughly distinguish two cases: discrete coupling, which can be generated locally at fiber splices and connectors caused by imperfect unions of fiber ends, and continuously-generated coupling along the fiber

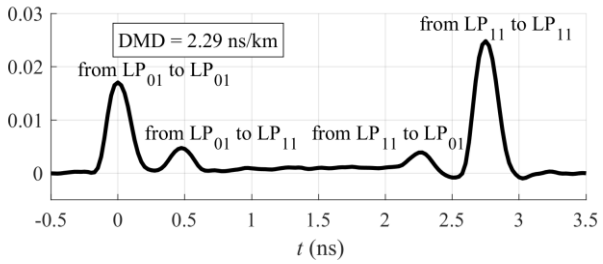

Fig. 2. Received signal corresponding to a single pulse propagated trough a link of Corning SMF-28e composed of 1 km connected through an optical connector to a 200 m span.

length, due to index profile imperfections, twists and bends of the fiber on all spatial scales.

The influence of continuous mode coupling in SSMF is minimized because of two main reasons [17]. Firstly, the two propagated modes couple weakly between each other as their propagation constants are not equal; indeed, both modes belong to different mode groups. The other reason is the limited length of passive fiber links at 850 nm due to the relatively high insertion losses (1.8 dB/km).

The optical power transfer suffered by a transmitted single pulse due to discrete mode coupling in an optical connector located between two SMF-28e fiber spans of 1 km and 0.2 km, is shown in Fig. 2. At the end of the first fiber span of 1 km, the propagated signal formed by two contributions, corresponding to each propagated mode like the examples in Fig. 1, couples to the modes that will propagate over the second fiber span of 200 m, as labeled in Fig. 2, to generate, at the output of the second span, one signal formed by 4 contributions with different relative delays. The first contribution corresponds to the signal propagated only on LP_{01} mode over both spans, in a similar way as the last contribution which has only propagated on the LP_{11} mode. The second and the third contributions result from the power interchange between different modes due to the fiber misalignment in the intermediate connector.

For the purpose of characterizing the fiber misalignment in a typical SC connector we have used a fiber setup composed by a patchcord of HI-780 fiber from Corning which is connected to a 680 m SMF-28 fiber span by means of a SC-UPC optical connector (see schematic included in Fig. 3). HI-780 is single-mode at 850 nm and, in a perfectly aligned junction with a SSMF span, the power carried by its fundamental mode would couple only with the LP_{01} mode of the SSMF, which would correspond with an MR = ∞ over the SSMF.

In a realistic connection, connector misalignment induces excitation of LP_{11} mode. Thus, when single pulses are transmitted and the MR on the received signal after the SMF-28 span is measured, as in Fig. 1, the magnitude of that misalignment could be derived, if the relation between connector misalignment and modal excitation in SSMF were known. We will assume that the unique origin of degradation in a non-ideal connector is lateral offset (as in [18]), which is entirely defined by radial offset (r_0), angular offset (φ_0) and angular rotation (φ_i,) as depicted in Fig. 3. However, because the fundamental mode propagated over HI-780 has a shape similar to LP_{01} mode propagated over SSMF, and the LP_{11} mode

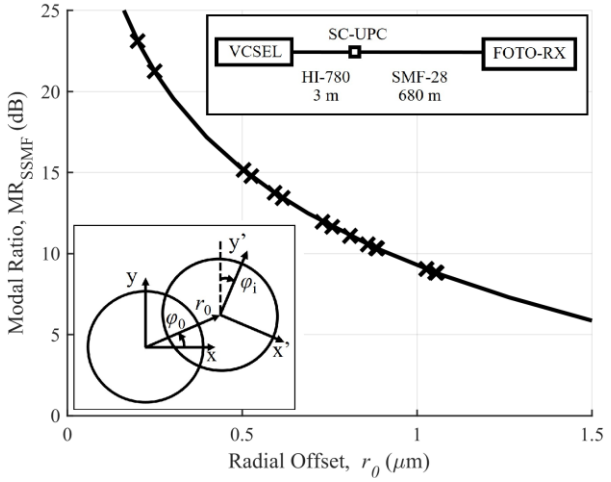

Fig. 3. Modal ratio of signal propagated over SMF-28 (MR_{SSMF}) as a function of radial offset (r_0) in a fiber interconnection with a HI-780: theoretical curve (solid line) and measurements (crosses). The schematic of the optical setup used for the measurements, and the coordinates systems and variables defining lateral offset between fibers are shown as insets.

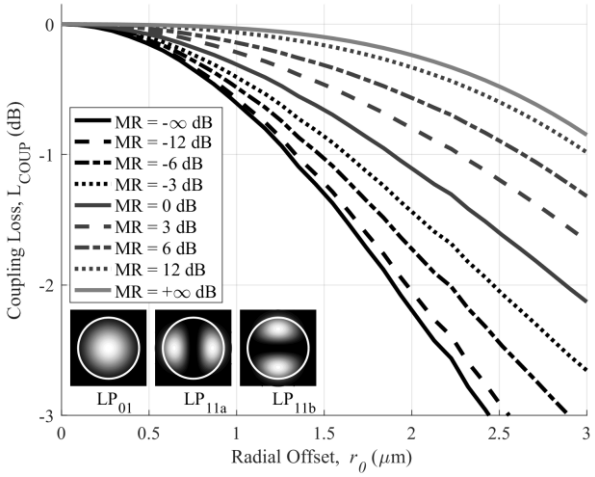

Fig. 4. Average coupling loss (L_{COUP}) due to radial offset (r_0) in a misaligned SMF-28 junction at 850 nm for different values of modal ratio of incident signal (MR), and normalized transversal power profiles of LP_{01}, LP_{11a} and LP_{11b} modes.

degenerates in two orthogonal components LP_{11a} and LP_{11b} (see modal power profiles included in Fig. 4), only r_0 has influence in varying MR in a junction between a HI-780 and a SSMF. The mode profiles for both fibers are calculated attending to their data sheets provided by Corning for a step-index profile (SMF-28: $n_1 = 1.4577$, $n_2 = 1.4525$, $2a = 8.2$ μm; HI-780: $n_1 = 1.4577$, $n_2 = 1.4525$, $2a = 4.0$ μm). The theoretical coupling coefficients, as a function of r_0, between the fundamental mode propagated over HI-780 and each mode of SMF-28 are obtained by integration of the corresponding transversal modal fields [19] and is showed in the Appendix. Thus a direct relation between measured MR and r_0 is established, as shown with the solid line in Fig. 3. The MR was measured for different SC connectors and the measurements results (marked with crosses in Fig. 3) are translated to r_0 values according to the theoretical curve. Thereby, the several derived r_0 values, from MR

measures of different installed fiber setups, present a mean value of 0.74 μm with a standard deviation of 0.28 μm. In [18] it is shown that r_0 can be properly modeled with a Rayleigh distribution. Thereby, the several derived r_0 values, from MR measurements, shown in Fig. 3 can be fitted to a Rayleigh distribution with a 0.55 μm scale parameter.

Besides the modal excitation, the lateral misalignment in an imperfect junction between two SSMF spans can also cause power loss when the incident light carried by incoming fiber cannot couple entirely to the propagated modes over the outgoing fiber. To evaluate this effect, the coupling coefficients between the fields of modes propagated over two misaligned SMF-28 spans have been computed similarly as it was made for Fig. 3 (see Appendix). In Fig. 4, the different curves, corresponding each one to a given MR value over incident fiber, show the coupling loss (L_{COUP}) as a function of r_0, and each point of those plots is obtained by averaging between 1000 realizations for a uniform distribution between 0 and 2π of φ_0 and φ_i, and also for the phase difference between incoming modal fields. When computing the optical power of the outbound coupled modal fields we consider both the incoherent terms, which are proportional to the power of the incident modes, but also the coherent terms, that result from the interference between the inbound modal fields and depend on its phase difference [20]. Fig. 4 shows that the averaged L_{COUP} is conditioned by the degree of misalignment but also by the relative level between the incident modes: for a given r_0, the losses increase with the relative level of LP_{11} mode with respect to LP_{01} mode. This effect is understandable if we take into account the intensity distribution in the transverse plane of LP_{11} mode, either LP_{11a} or LP_{11b}, which propagates more externally over SSMF than LP_{01} does (see profiles included in an inset in Fig. 4).

From these results, the effect of a single connector is fully characterized in terms of modal coupling and optical losses for any given incoming excitation (MR value and relative phase shift). In order to calculate the expected optical losses of a typical SC connector, the statistical distribution of lateral misalignment must be also considered. The lateral misalignment r_0 can be properly modeled with a Rayleigh distribution, whereas a uniform distribution between 0 and 2π is used for φ_0 and φ_i. Numerical simulations have been carried out to quantify the coupling loss associated to this configuration but considering also the mode excitation. The average coupling loss of an optical connector has been calculated over 10,000 realizations for an incident signal with uniform distribution of MR between −15 and 15 dB, considering both the coherent and incoherent terms of modal coupling as it has been done previously when calculating L_{COUP} for Fig. 4. The mean loss obtained for a single connector is 0.2 dB which is a typical value for factory-polished optical connectors designed to minimize reflectance loss. Thus, the connector characterization derived in this section, which has been developed using the well-established model of fiber misalignment in [18] and complemented by our measurements, is suitable for being used in subsequent sections to simulate SSMF interconnections.

C. Mode Filtering

In a bimodal propagation scenario, the effectiveness in reducing the induced ISI by filtering the only high order mode (HOM) is clear. Specifically for SSMF at 850 nm, there are many examples of mode filters based on diverse techniques: tapered-fiber [12], sub-wavelength optical wire [21], mode coupler [3], or single-mode fiber at 850 nm [13], [15]. Furthermore, a simple MF constructed by coiling properly the end-tail of the fiber span provides high performance in rejecting propagated HOM as in [10]. For the SMF-28 example in Fig. 1a, by coiling 4 loops of the fiber end-tail with a 10 mm diameter a mode suppression ratio (MSR) about 18 dB with 0.1 dB of insertion loss (IL) were obtained; both values defined in terms of optical power as: $MSR = MR^{OUT} / MR^{IN}$, $IL = P_{01}{}^{IN} / P_{01}{}^{OUT}$. For the ESSMF in Fig. 1b, the diameter of the loops was reduced to 6 mm to achieve an MSR = 22 dB with IL = 0.5 dB.

However, the main drawback associated to MF is the need to include a filtering element just before whatever point of the link that could potentially induce mode coupling. As it was shown in Fig. 2, in a link composed by two fiber spans, the mode coupling produced in the connection between spans adds additional ISI contributions at the end of the fiber link. For a complete removal of that ISI, the inclusion of a MF at the end of each fiber span is required. If the MF's were included just at the end of the last span, it would only attenuate the signal contributions propagated over LP_{11} mode in this last span (the second and fourth contributions in Fig. 2), but the third contribution, that also generates ISI, would remain unaltered as it was propagated over LP_{01} along this last span.

III. Signal Equalization

The equalizers used in this work are based on a T/2 fractionally-spaced minimum mean square error (MMSE) DFE. This structure is composed by a feed-forward filter (FWF) of $K_w + 1$ coefficients that operates on the signal sampled at twice the symbol rate, and a feed-back filter (FBF) of K_b coefficients working at baud-rate, this scheme is widely described in the literature [22][23], and its schematic is shown in Fig. 5a. In this work, the BER provided by the different equalizers is estimated by quasi-analytical method, which consists in simulating the overall model without the noise contribution (additive white Gaussian noise, AWGN, in this case) to generate the overall ISI caused by the global channel, and then the filtered noise statistical effect, that is, its analytically derived autocorrelation, is added to obtain the error rate, as is explained in detail in [24]. Therefore, the high computational complexity associated to the estimation of very low BER values by error counting (Monte Carlo method) can be significantly reduced: for instance in this work, sequences of 10^4 bits are long enough to reliably estimate BER values around 10^{-12}, whereas for an accurate estimation by Monte Carlo method length sequences much longer than 10^{12} would be needed. This efficient method of BER estimation is also employed in the 10GBASE-LRM interface of the 10GbE standard [1] to estimate by simulation the dispersion penalty provided by a DFE [25]. Moreover, when the BER of DFE and

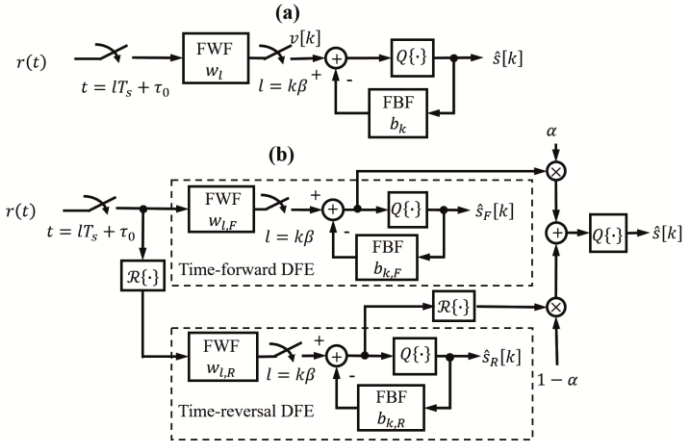

Fig. 5. Block diagrams of DFE (a), and STR-DFE/LC-BiDFE (b) equalizers.

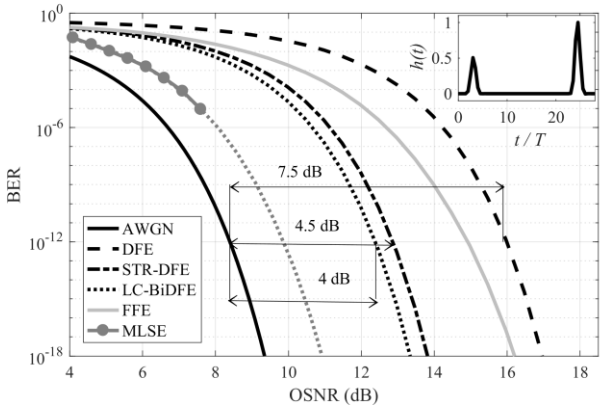

Fig. 6. BER as a function of OSNR for MLSE, FFE, DFE, STR-DFE and LC-BiDFE receivers, for the simulated channel impulse response, *h(t)*, included in the inset.

BiDFE schemes is estimated by quasi-analytical method, we assume no-error propagation across FBF, which is reasonable because of the target BER (10^{-12}), as in 10GBASE-LRM [1], [25].

With the purpose of illustrating both the limited performance of the classical DFE and the capabilities of the proposed BiDFE schemes, Fig. 6 shows the BER curves for an example of a performance limiting channel in terms of ISI. In this case, a 1 km single span link of SSMF produces a channel impulse response with two main contributions, each one associated directly to a propagated mode, as the ones shown in Fig. 1. The simulated channel impulse response, included in the inset, is formed by two contributions, where the first has half the maximum amplitude of the second. The BER curves obtained after using an equalizer are plotted as a function of the signal to noise ratio in terms of optical power (OSNR) and are compared to an ideal loss-less AWGN channel, which is equivalent to a channel without ISI, and is plotted with a solid line in Fig. 5.

A. Decision Feed-back Equalization

DFE, despite being suboptimal from the point of view of error probability, offers an effective and low complexity solution to combat ISI. To constrain receiver complexity the FWF order (Kw) has to be limited, while the FBF order (Kb) must be as long as the most delayed path.

To compensate a channel impulse response with two contributions clearly separated in time (like those showed in Fig. 1), an ideal DFE (with infinite filters length) operates as follows: the FWF generates an equivlent channel impulse response with most of its energy concentrated at the beginning, or in other words, it generates a minimum-phase equivalent channel; then, the FBF eliminates the ISI due to previously detected symbols. On the other hand, a DFE designed with a FWF of only one coefficient ($K_w = 0$) and a FBF order long enough to achieve the maximum channel delay, can only select the maximum amplitude tap of the channel impulse response and then cancel the ISI generated by taps after the selected one (cursor). Therefore, in this case, the signal power at the output of the FWF is maximized, but at the expense of making impossible to compensate the ISI of the taps in the channel impulse response previous to the cursor, that is, the ISI generated by symbols which have not been detected yet and that cannot be eliminated by the FBF [5].

In this work, a low complexity DFE configuration has been used, where the FWF order is much lower than the maximum delay induced by the channel ($K \gg K_w$). This configuration is closer to the single tap FWF operation, although it allows to compensate some contribution of the pre-cursor ISI by means of the FWF. Therefore, the equalizer operates detecting the symbol associated to the strongest tap of the first contribution of the channel impulse response. For instance, in Fig. 1a, it corresponds to the tap at $t = 0$ of mode LP_{01}: the FWF can compensate the ISI due to taps around $t = 0$ caused by limited system bandwidth and/or GVD, while FBF combats the ISI of taps for $t > 0$ mainly caused by modal dispersion. As a result, the signal to noise ratio (SNR) at the output of the equalizer is dominated by the amplitude level of the first signal contribution of the channel impulse response. The filters configuration for all equalizers used in this work makes use of a FWF order $K_w = 4$, as it provides a good trade-off between performance and complexity, and a FBF length that is adjusted to cope with the dispersion induced by the SSMF.

For the example in Fig. 6, it is shown how the BER curve converges for the DFE (dashed line) with $K_w = 4$ and $K_b = 25$ (the same filters configuration is used in the remaining DFE-based equalizers in this section), that is, it can cope with the ISI induced by the second contribution of the channel impulse response, but it requires a high OSNR to achieve lower values of BER. The reason for this poor performance is because most of the energy of the channel impulse response is in the second contribution. For example, an OSNR = 16.1 dB is required to obtain a BER = 10^{-12}, which implies an optical power penalty with respect to the loss-less AWGN channel of 7.5 dB.

B. Selective Time-Reversal DFE

As noted previously, DFE BER performance is degraded when the channel impulse response has last taps with higher levels. To solve the equalization of those cases, we make use of a time-reversal solution: by reversing in time the order of the received samples, the equivalent channel impulse response becomes a time-reversed version of the actual channel impulse response: $\hat{h}(t) = h(-t)$ [20]. The main drawback of working with

TABLE I
COMPLEXITY OF EQUALIZERS

Receiver	General expression of the number of Mult/Adds operations	Number of Mult/Adds operations for the example of Fig. 6
MLSE	$(K+1)\cdot M^K$	$8.72\cdot10^8$
FFE	$K_{ffe}+1$	51
DFE	$K_w + K_b+1$	30
STR-DFE	$K_{w,F} + K_{b,F}+1$ or $K_{w,R} + K_{b,R}+1$	30
LC-BiDFE	$K_{w,F} + K_{b,F}+1+ K_{w,R} + K_{b,R}+1$	62

the time-reversed version of the signal is the inherent latency associated: the entire signal has to be received previously to start its detection. However, the latency can be reduced by partitioning the received signal through windowing techniques, in exchange of a higher implementation complexity. For instance, if a typical Ethernet frame (1538 bytes) is taken as the signal unit, the latency associated to the use of a time-reversed version of the signal will be above 1.2 μm at the 10GbE line rate [26]. If this latency value were too large, the signal could be partitioned in shorter windows. Therefore, when the delayed mode is predominant in a SSMF link, the equalizer would work with the time-reversed data samples and then the delayed mode would become the first channel tap and so the second one would be the weakest one, giving the conditions where the DFE has better performance. This solution is called Selective Time-Reversal (STR-DFE): it alternates between time-forward and time-reversal operation as channel conditions benefit one or the other option to minimize the MSE of equalized symbols. The block diagram is shown in Fig. 5b, taking into account that the value of the coefficient α can only be 0 or 1, as it operates as selector.

In the example of Fig. 6, STR-DFE (dot dashed line) operates in time-reversal operation mode and its OSNR penalty with respect to AWGN channel becomes 4.5 dB. The improvement from operating in time-reversal compared to time-forward (conventional DFE) is 3 dB in optical power units.

C. Linear Combining Bidirectional DFE

The bidirectional DFE (BiDFE) structure combines the outputs of a time-forward with a time-reversal DFE's to reduce overall noise enhancement at the equalizer output, as is shown in Fig. 5b where the coefficient α can take any real value between 0 and 1. As the FWF filtered noise from the two equalized output flows are uncorrelated, the overall SNR improves when these outputs are added. There are different schemes to combine both equalized outputs. In this work, we have made use of a linear combiner as proposed in [21], giving the Linear Combining BiDFE (LC-BiDFE). Both flows are added after being weighted depending on their own MSE exploiting the inherent diversity between both equalizers to decrease the noise gain term and the residual ISI component of the combined output.

In the example of Fig. 6, the LC-BiDFE operates by balancing the weighting toward the time-reversal DFE output (approximately 80% of the total output), as it provides lower BER, but avoiding the suppression of the time-forward DFE (around 20% of total) to obtain an overall noise reduction. Thereby, the LC-BiDFE (dotted line) provides an OSNR penalty from AWGN channel of 4 dB which implies a further reduction of 0.5 dB compared with the STR-DFE.

D. Complexity of the Equalizers

In this section, the complexity of different receivers is estimated by computing the number of operations, additions and multiplications, required to detect one symbol.

Firstly, the Maximum Likelihood Sequence Estimator (MLSE) is the optimum receiver since the point of view of minimizing the error probability; its great detection performance can be appreciated in the example of Fig. 6 (line marked with circles), where the MLSE provides a BER curve very close to the curve of the AWGN channel. However, MLSE, even if the efficient Viterbi algorithm is implemented, has a complexity that is exponential with the channel memory (maximum channel delay in symbol period units or order of the channel impulse response, K) [22]: $(K+1)\,M^K$, being M the constellation size of the modulation. For the example of Fig. 6, the channel memory is K =25, and the OOK modulation implies that M = 2; so, the required complexity is $8.72\,10^8$ multiplications and additions.

The T/2 fractionally-spaced Feed-Forward Equalizer (FFE) is a linear equalizer that enables a symbol-by-symbol detection; it is formed by a FIR filter of order K_{ffe} that operates on the received signal at twice the symbol rate. The complexity associated to the filtering operation is proportional to the length of the filter: $K_{ffe}+1$. For the example of the Fig. 6, a FFE (the solid gray line) with $K_{ffe} = 50$ is used, which requires computing 51 multiplications and additions.

The complexity of the DFE is obtained summing the complexities of the FWF and the FBF: $K_w + K_b+1$, for the example are needed 30 multiplications and additions.

Regarding to BiDFE receivers, the STR-DFE complexity depends on the operation mode selected, time-forward or time-reversal, and more specifically to the filter configuration of each stage. In this work, the same configuration in both stages is assumed, which is also the same as the one used by the DFE receiver ($K_{w,F} = K_{w,R} = K_w$ and $K_{b,F} = K_{b,R} = K_b$), therefore the example complexity is the same as the DFE case. Finally, as the LC-BiDFE makes use of two DFE's and a weighting of each output, 62 multiplications and additions are needed in the example.

As a summary, the estimated complexity of the receivers is shown in Table I. For the example simulated, it can be seen that the MLSE, though providing the best BER performance, it has a prohibitive complexity due to the high dispersion delay induced by the channel. In comparison, the FFE complexity is drastically reduced, but also its performance. The DFE complexity is slightly higher to half the one of the FFE, although for this example, which is especially challenging for this kind of receiver, its BER performance is worse. However, in this example, a STR-DFE operating in time-reversal mode has the same complexity as the DFE, but the obtained BER is lower than that of DFE and FFE receivers. Finally, the

LC-BiDFE has a complexity slightly higher than the FFE one, but it provides the best BER performance excluding the MLSE.

Nevertheless, it should be pointed out that in the DFE hardware implementation there is a remarkable difference between the FWF and the FBF in terms of complexity. As the FBF operates on detected and quantified symbols, they only can take values from the finite alphabet modulation constellation (in this work ±1). Thus, the FBF convolution operation can be performed exclusively by addition and subtraction operations, which are significantly less costly (in area and power consumption) than multiplications between real numbers as the ones done by the FWF, and also the FFE. As a consequence, even though the FFE and the LC-BiDFE require a similar complexity, as the FFE filter length is about 5 times longer than the two FWF's of the LC-BiDFE, in a real implementation, LC-BiDFE would need much less resources. Moreover, due to the characteristic shape of the channel impulse response induced by the SSMF, we have found that most of FBF coefficients are zero valued: for the example shown in Fig. 6, only 5 of the 25 coefficients of each FBF have values > 10^{-4}. This feature can be exploited to reduce the FBF operations and hence the required complexity in Table I would be further reduced.

IV. Extended SSMF Reach by Equalization

In this section, the influence of the VCSEL source and the main SSMF features affecting the propagated signal, which have been characterized in section II, are jointly evaluated by means of numerical simulations to calculate the reach improvement provided by the equalizers. Firstly, a system formed by a single SSMF span without any connector is simulated in order to separately assess the effect of modal dispersion (see Fig. 7a). Secondly, the fiber optic cabling model used in [1] is constructed, including also the optical connector misalignment distribution derived in section II.B, to evaluate the coverage improvement provided by the equalizers; this model consists of a single span of SSMF connected to front ends by respective 3 m length SSMF patchcords (see Fig. 8a). With respect to the optical source, two types of VCSEL have been considered in the simulations: single-transverse mode (STM) and multi-transverse mode (MTM). A VCSEL with an active area diameter lower than 5 μm generates only one transverse mode (STM) at 850 nm with a quasi-Gaussian shape and a typical linewidth lower than 100 MHz. On the other hand, for higher diameter of the active region, the VCSEL generates many transversal modes (MTM) and an emission spectrum with multiples peaks.

The simulation model consists of a VCSEL at 850 nm that illuminates a SSMF link for a given MR with a fixed transmitted optical power and fiber loss of 1.8 dB/km where the non-linear effects are neglected. The intensity modulated and direct detected (IM/DD) optical link includes a transmitter electrical Gaussian filter with step response $T_{20\text{-}80\%}$ = 47 ps, and a receiver electrical Bessel filter of 4th order with a 7.5 GHz cut-off frequency, like those used by 10GBASE-LRM [1, Clause 68] to evaluate MMF links. Only thermal and shot noises are considered and they are modeled as a unique source of AWGN. The noise power value at the receiver is fixed and characterized in optical power units as Noise Equivalent Power (NEP) of NEP = 22.7 pW/$\sqrt{\text{Hz}}$. The optical power of the VCSEL is adjusted to obtain a given value of OSNR by means of:

$$OSNR = \frac{OMA}{2 \cdot NEP \sqrt{BW_{eq}}} \quad (1)$$

Where the Optical Modulation Amplitude (OMA) of the VCSEL is defined as the difference between the optical power levels of the OOK modulated optical signal (OMA = $P_1 - P_0$), and BW_{eq} is the equivalent bandwidth of the receiver electrical filter. Optical power penalties (including loss) with respect to the AWGN case (for a BER = 10^{-12}) have been obtained (see Fig. 6) to evaluate the equalizers described in section III. The maximum penalty allowed when considering the feasibility of the equalizers is 6.5 dB, which is the same allocated penalty for dispersion in 10GBASE-LRM except that here the fiber losses are also included. The higher absorption losses of the SSMF at 850 nm and the longer link lengths studied in this work requires including this more restrictive premise to evaluate more accurately the maximum reach attained.

A. Single Transversal Mode VCSEL and Single SSMF Span

Firstly, the mode excitation due to the VCSEL launching and the SSMF induced mode delay (the sign of DMD mainly) need to be jointly analyzed to assess how these parameters would affect the link performance. In order to avoid any modal coupling, no connectors will be included in this first setup. We make use of the model included in Fig 7a consisting of a single span of 2 km length for two different SSMF types and a STM-VCSEL as optical source. The use of a STM-VCSEL implies that the spectral bandwidth of a modulated optical signal will depend mainly on the transmitted bit rate. Thus, for the simulations performed in this section, the influence of GVD is diminished: a pulse at 10 Gb/s propagated exclusively over LP_{01} or LP_{11} mode would suffer a time broadening lower than 1 % after a 2 km SSMF link.

Fig. 7b shows the power penalties for the Corning SMF-28 case. In this link, a conventional receiver (dotted line) would be feasible if the strongest mode is at least 11 dB over the weakest one, regardless of which one (LP_{01} or LP_{11}) is higher; under this condition the level of the ISI would not disturb data detection. If a MF is added before the photoreceiver, the LP_{11} mode is cancelled and ISI disappears, then the feasibility of the link would depend on the remaining LP_{01} mode signal power. In this case, the link would be feasible only if the LP_{01} is excited with 8.5 dB over the LP_{11} (dashed line). Therefore, compared with the conventional receiver, MF can extend positive MR range operation at the expense of loss of feasibility for negative MR values, and this behavior does not change if an ESSMF from Draka is used instead, as shown in Fig 7c. In brief, for a 2 km link length the use of a conventional receiver, with or without a MF, requires a quite pure single mode excitation.

If a DFE stage is used, the simulation results in Fig. 7b (dot dashed, which is partly covered by the light solid line) show that the link would be feasible only when the LP_{01} were 2.5 dB

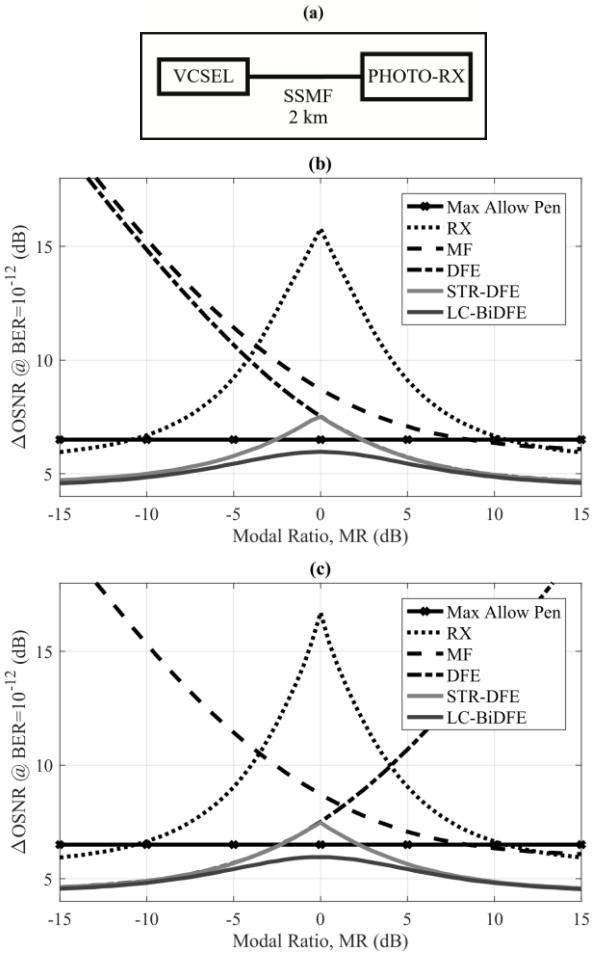

Fig. 7. Power penalties to achieve a BER=10^{-12} depending on MR in a 2 km SSMF single span link (a) for Corning SMF-28 (b) and Draka ESSMF (c). Signals corresponding to received (RX), mode filtered received (MF), and DFE, STR-DFE and LC-BiDFE equalized.

stronger than $LP_{11,}$ for an equalizer configuration with $K_w = 4$ and $K_b = 49$. Although the DFE cancels the ISI over the first strong tap associated to LP_{01} mode, when the level of this tap decreases the effective SNR at the equalizer output is reduced accordingly, and thus the overall performance tends to be the same as the MF for negative values of MR. When the fiber considered is the Draka ESSMF, the results shown in Fig. 7c are obtained. These results are similar to the ones obtained for the SMF-28 fiber but in the DFE case the penalty response is inverted along the MR axis because the DMD is negative in this fiber; that is, the LP_{01} mode arrives now after the LP_{11} mode. Additionally, the FBF order required is lower since the DMD is also lower: $K_b = 10$ for ESSMF.

It is clear from both results that the DFE receiver would fail in those cases when the strongest mode is the delayed one or the power levels of both modes are similar. STR-DFE alternates between time-forward and time-reversal operation as channel conditions benefits one option or the other. In Fig. 7b, STR-DFE (the light solid line) applies time-forward (equivalent to conventional DFE) for positive MR values and time-reversal for negative ones. An equivalent behavior is shown in Fig. 7c for the ESSMF fiber but interchanging the operation mode; in all cases STR-DFE provides penalty compliance for MR values higher than 2.5 dB or lower than −2.5 dB.

However, the STR-DFE fails when the levels of both modal contributions are similar. When the MR is around 0 dB LC-BiDFE (the dark solid line in Fig. 7) combines the outputs of time-forward and time-reversal DFE's by weighting equally both flows, and the reduction of penalty with respect to time-forward or time-reversed DFE single equalizer is maximum. As the MR value rises in positive or negative sign the combiner distributes the weights among each flow and the performance of LC-BiDFE tends to be the corresponding to the STR-DFE operation mode. As shown in Fig. 7 full penalty compliance is assured for both SSMF types whatever the modal ratio.

In this section, it has been shown that the capability of processing the time-reversed version of the received signal allows STR-DFE and LC-BiDFE to deal with the positive and the negative sign of DMD alike. Moreover, those equalizers can cope equally with any value of DMD of the SSMF if the FBF order is adjusted to be as long as the maximum modal delay. Therefore, only the SMF-28 will be evaluated hereafter in this work since the results obtained by the equalizers can be extrapolated to other SSMF with different DMD values.

B. Single Transversal Mode VCSEL and SSMF Cabling Model

To evaluate the reach provided by the equalizers in a realistic installation including the effect of modal coupling, the SSMF cabling model is constructed by adding two misaligned optical connectors in both junctions between the fiber span and each patchcord at the fiber ends, as shown in Fig. 8a. In each simulation, the fiber link of length L_{TX} is illuminated by a STM-VCSEL to produce a mode excitement given by MR_{TX}, and the corresponding OSNR penalty is calculated. For each L_{TX} and MR_{TX} values, 5000 realizations are carried out to evaluate the effect of statistical misalignment of the optical connectors, which are modeled as explained in section II.B. The results presented in Fig. 8 show the computed cumulative density function (CDF), over all realizations for each simulation, of OSNR penalties below 6.5 dB for five cases: received signal (Fig. 8b), received signal including MF just before each connector (Fig. 8c), and received and equalized by DFE (Fig. 8d), STR-DFE (Fig. 8e) and LC-BiDFE (Fig. 8f). In all cases, an isoline of CDF = 99 % is plotted as we consider that percentile as the threshold to assess the feasibility of the link.

When comparing this system with the single SSMF span, without optical connectors, there are two main distinctive implications which remain valid for all receivers. On the one hand, the combined effect of modal coupling at the connectors and a coherent source, as the STM-VCSEL, generates at the photoreceiver some coherent terms that contribute to a further degradation of the detected signal. As it was explained earlier

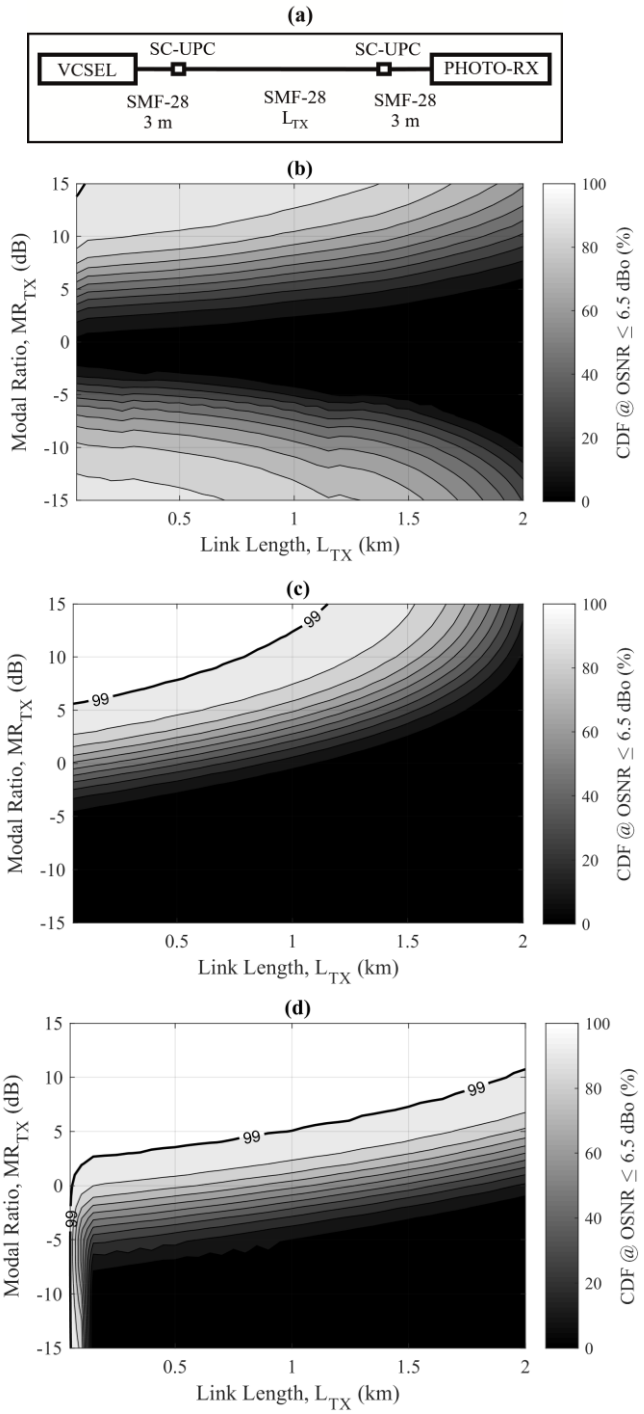

in section II.B, these terms origin from the beating between coupled modal fields and they are also dependent on the phase difference between them [20], and thus, unlike the incoherent terms, those terms cannot be fully compensated by equalization due to their non-direct dependence with the optical power of the propagated modes. On the other hand, the effect of increasing modal coupling loss for lower levels of MR_{TX} (as shown in Fig. 4) produces worse receiver performance for the negative range of MR_{TX} than for the positive one.

The conventional receiver detects directly the signal propagated along the SSMF link, and its corresponding CDF results in Fig. 8b show a very poor performance; this receiver is only feasible (CDF ≥ 99 %) if the LP_{01} mode is much more

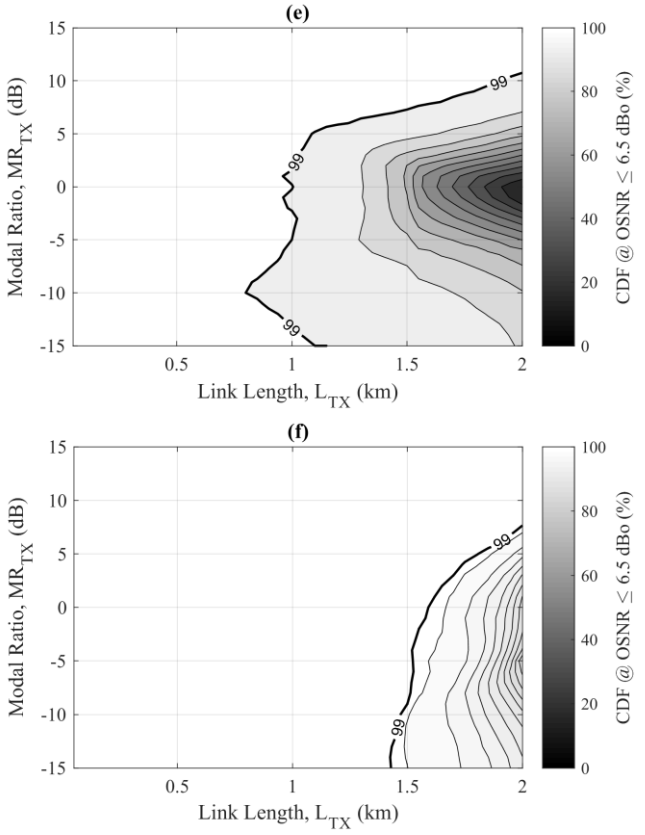

Fig. 8. CDF of OSNR penalties with respect to AWGN lower than 6.5 dB to obtain BER = 10^{-12} of 5,000 realizations for each given modal ratio (MR_{TX}) and length of SSMF single span (L_{TX}) of cabling model including patchcords in both ends and a STM-VCSEL (a). Results correspond to only received signal (b), received including MF just before each connector (c), and received an equalized by DFE (d), STR-DFE (e) and LC-BiDFE (f).

excited than the LP_{11} mode (for $MR_{TX} \geq 14$ dB). The maximum coverage with the conventional receiver is just 100 m when $MR_{TX} = 15$ dB. If a MF (Fig. 8c) is inserted just before each optical connector, the system can extend its valid operation range, both in MR_{TX} domain and maximum reach: it is feasible for $MR_{TX} \geq 6$ dB, achieving a maximum reach of 1.15 km for $MR_{TX} = 15$ dB.

If DFE processing is applied to the received signal (Fig. 8d), the reach is clearly increased compared to the conventional receiver (with or without MF) but the system performance remains strongly limited for negative values of MR_{TX}. Thus, the coverage obtained exceeds 2 km for $MR_{TX} = 15$ dB, but it is reduced progressively for lower values of MR_{TX} achieving a minimum reach of 50 m around $MR_{TX} = -6$ dB, distance which is maintained up to $MR_{TX} = -15$ dB.

The possibility of choosing the time-reversal operation of DFE by using STR-DFE (Fig. 8e) benefits coverage for negative values and around 0 dB in MR_{TX} range whereas maintains the reach for positive MR_{TX} values. STR-DFE presents a minimum reach of 0.8 km for $MR_{TX} = -10$ dB extending the coverage up to 1.15 km for $MR_{TX} = -15$ dB. The combined effect of coupling loss and non-linear interference causes the asymmetrical behavior of STR-DFE compared to the results in Fig. 7, where the worst case corresponded to MR = 0 dB.

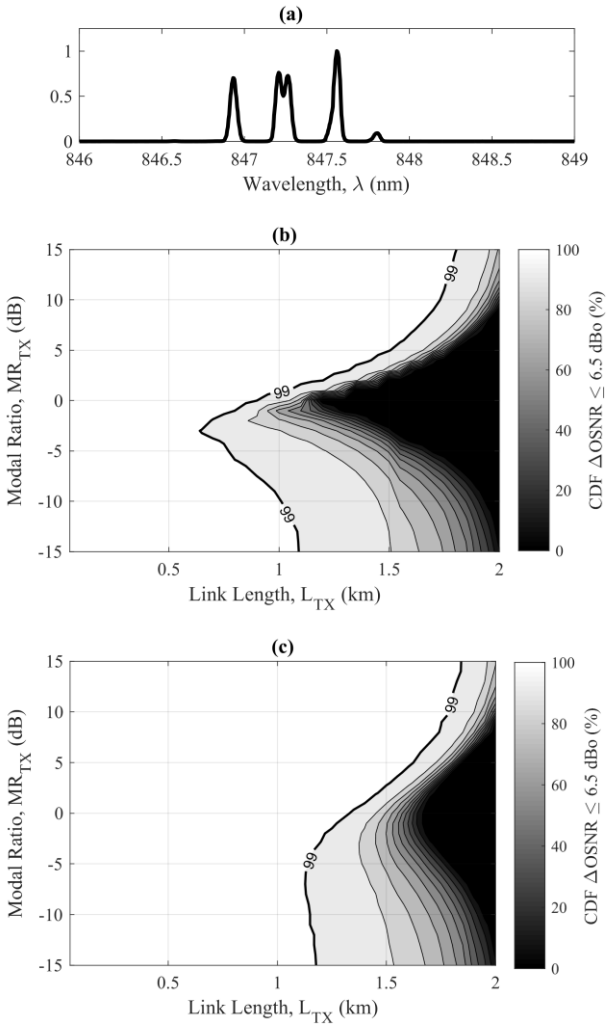

Fig. 9. CDF of OSNR penalties with respect to AWGN lower than 6.5 dB to obtain BER = 10^{-12} of 5000 realizations for each given modal ratio (MR_{TX}) and length of SSMF single span (L_{TX}) of cabling model including patchcords in both ends and a MTM-VCSEL whose spectrum is showed in (a). Results correspond to signal received and equalized by STR DFE (b) and LC BiDFE (c).

Finally, combining the outputs of both DFE operation modes (time-forward and time-reversal), LC-BiDFE (Fig. 8f) extends the coverage provided individually by each operation mode. Compared with STR-DFE, the reach improvement is achieved both in positive MR_{TX} range, 2 km is attained for MR_{TX} = 8 dB, and in negative range, 1.45 km for MR_{TX} = −15 dB. Moreover, as previous results in Fig. 7, the improvement of LC-BiDFE with regard to STR-DFE is maximized for MR_{TX} values around 0 dB; here, LC-BiDFE exploits the inherent diversity between both equalized flows and even the non-linear interference could be partially cancelled as the residual ISI of both outputs are uncorrelated. Nevertheless, the effect of higher coupling loss for lower MR_{TX} values, implies again shorter reach results for negative values of MR_{TX}, and now the minimum coverage achieved is 1.45 km at MR_{TX} = −14 dB. These results confirm that the LC-BiDFE receiver is able to effectively increase the coverage of a SSMF link at 850 nm for any launching condition of the STM-VCSEL.

C. Multi-Transversal Mode VCSEL and SSMF Cabling Model

In this section, the use of a MTM-VCSEL source in the SSMF cabling model shown in Fig. 8a will be analyzed. The CDF results of STR-DFE and LC-BiDFE receiver are shown in Fig. 9, where the optical power spectrum is also plotted. The use of a MTM-VCSEL as optical source combined with the high value of DMD of SMF-28 fiber has as a consequence that IM/DD system is considered incoherent [27]. In general terms, the product of the differential delay between the components of any wave and the bandwidth of the optical source that generates that wave defines an incoherent interaction if the following relation is satisfied: $\Delta\tau \cdot \Delta f > 1$. The considered MTM-VCSEL has a separation between its spectral components of approximately 0.4 nm (see Fig. 9a) and, taking into account the DMD of a SMF-28, the modal interaction would be considered incoherent for a length of fiber L > 2.8 m, which is typically the length of a patchcord. However, it should be noted that the results of coupling losses presented in section II remain equally valid for an incoherent system. Moreover, the several peaks of the MTM-VCSEL spectrum contribute to a non-negligible GVD. For the spectrum of Fig 9a and for a 2 km link length, a 10 Gb/s pulse would suffer a time broadening higher than 30 %.

The incoherence of the source causes that there are no beating coherent terms at the photoreceiver, and the remaining incoherent terms can be properly compensated by the equalizers. With all these effects combined, both equalizers present worse results around MR_{TX} = 0 dB, as occurred in Fig. 7 in a scenario where there were no connectors, although now the coupling losses cause that the minimum reach is obtained for negative values of MR_{TX}, as in previous results. However, the results present a reduced coverage compared to using a STM-VCSEL as in Fig. 8 due to GVD. Even though the DFE-based equalizers can cancel the ISI induced by GVD, as was mentioned in section III.A, the SNR of the equalized signal becomes reduced due to the noise enhancement induced by the FWF compared to the previous case with negligible GVD.

From Fig. 9, STR-DFE presents a minimum reach of 0.65 km for MR_{TX} = −3 dB, achieving 1.8 km for MR_{TX} = 15 dB and 1.1 km for MR_{TX} = −15 dB. LC-BiDFE achieves at least 1.15 km, for MR_{TX} = −7 dB, and 1.85 km and 1.2 km, for MR_{TX} = 15 dB and MR_{TX} = −15 dB respectively.

V. Remarks and Conclusion

The combination of a VCSEL operating at 850 nm with the use of SSMF as transmission mean has been analyzed. The main perturbation of the link arises from the bimodal propagation, which have been shown to present heterogeneous behavior in modal propagation at 850 nm, both in magnitude and sign of DMD. It has been found that the channel impulse response is conditioned not only by the VCSEL launching condition but also by the DMD sign of the SSMF. Also, it has been shown that the modal coupling induced by misaligned optical connectors in the link can severely degrade the transmitted signal, bringing about additional interference and losses to those generated by the

SSMF itself. A model has been derived to calculate statistically the coupling losses and modal coupling in an optical connector due to lateral misalignment. This model has been used in the SSMF cabling model simulations.

The conventional receiver combined with mode filtering has been proved to be limited in combating modal dispersion, especially when mode LP_{11} gets more strongly excited than LP_{01} by the VCSEL source. Besides, it would be difficult to implement it in legacy SSMF links as it requires including a filter just before each connector in the link. The classical DFE processing has also exhibited poor performance when the channel conditions generate a channel impulse response that has most of its energy in the delayed taps.

The implementation of time-reversal operation allows STR-DFE and LC-BiDFE equalizers to deal with modal dispersion for whatever DMD value, if the FBF order is high enough to compensate the maximum modal delay induced by the SSMF. However, LC-BiDFE presents the best performance as it combines outputs of both time-forward and time-reversal operation to reduce overall noise gain and residual ISI term. Thus, the LC-BiDFE assures a 1.45 km minimum reach at 10 Gb/s for all fiber excitement conditions in a realistic single span SSMF link with patchcords in both ends and using a STM-VCSEL, where the effects of mode coupling and insertion loss induced by optical connectors are taken into account. If a MTM-VCSEL is used instead, the effect of GVD becomes significant and the minimum reach provided by LC-BiDFE is reduced slightly but a distance of 1.15 km is still attained.

APPENDIX

In this section, the modal coupling in a laterally misaligned junction between two step-profile optical fibers under weakly guidance is modelled [19].

In the interface of two fibers, the transversal field components fulfill the continuity condition:

$$\vec{E}_{t,in} = \vec{E}_{t,out} \qquad \vec{H}_{t,in} = \vec{H}_{t,out} \tag{2}$$

In the incoming fiber the fields are a linear combination of the propagated modes:

$$\vec{E}_{t,in} = \sum_k c'_k \cdot \vec{e}'_{t,k} \qquad \vec{H}_{t,in} = \sum_k c'_k \cdot \vec{h}'_{t,k} \tag{3}$$

On the other hand, in the outgoing fiber, the fields are a combination of propagated modes, and radiated modes that vanish along the fiber:

$$\vec{E}_{t,out} = \sum_j c_j \cdot \vec{e}_{t,j} + \vec{E}_{t,rad} \qquad \vec{H}_{t,out} = \sum_j c_j \cdot \vec{h}_{t,j} + \vec{H}_{t,rad} \tag{4}$$

The coefficient that weights the j-th propagated mode at the output is computed by integrating over an infinity section the transversal field components at both sides of the discontinuity:

$$c_j = \frac{1}{2N_j} \int_{A_\infty} \vec{E}_{t,in} \times \vec{h}_{t,j} \cdot \hat{z}\, dA = \frac{1}{2N_j} \int_{A_\infty} \vec{H}_{t,in} \times \vec{e}_{t,j} \cdot \hat{z}\, dA \tag{5}$$

The normalization factor of the j-th mode is defined as:

$$N_j = \frac{1}{2} \int_{A_\infty} \vec{e}_j \cdot \times \vec{h}_j \cdot \hat{z}\, dA \tag{6}$$

The modal fields in a weakly guiding optical fiber have only transversal components ($E_z = H_z = 0$). For the case of an electrical field with linear polarization along the x axis, the modal field can be expressed as:

$$\vec{E} = e_x(x,y) \cdot \exp(i\beta z) \cdot \hat{x} \quad \vec{H} = n_1 \sqrt{\frac{\varepsilon_0}{\mu_0}} e_x(x,y) \cdot \exp(i\beta z) \cdot \hat{y} \tag{7}$$

In a lateral offset misalignment, the fibers are parallel to the propagation z axis without any gap between them, and thus the incident fields are totally transversal. Therefore, the modal amplitude corresponding to j-th propagated mode on the outgoing fiber is calculated by adding the results of integrating the transversal distribution of that mode and each propagated mode in the incoming fiber with amplitude c'_k:

$$c_j = \frac{1}{2N_j} \int_{A_\infty} \left[\sum_k c'_k \cdot e_{x,k}(x',y') \cdot \hat{x} \right] \times \left[n_1 \sqrt{\frac{\varepsilon_0}{\mu_0}} e_{x,j}(x,y) \cdot \hat{y} \right] \cdot \hat{z}\, dA = \tag{8}$$
$$= \sum_k c'_k \int_{A_\infty} e_{x,k}(x',y') \cdot e_{x,j}(x,y) \cdot dA$$

Where, for simplicity, we assumed that the modal field distributions are normalized in power:

$$\int_{A_\infty} \left| \vec{e}_{t,l}(x,y) \right|^2 dA = \int_{A_\infty} \left| e_{x,l}(x,y) \right|^2 dA = 1, \quad \forall l = 0,1,2,... \tag{9}$$

The field distributions of LP_{lm} modes, including both distributions as sine and cosine functions (LP_{lma} and LP_{lmb}), expressed in cylindrical coordinates with radial variable normalized to the core radius can be expressed as:

$$\vec{E}(R,\varphi,z) = \hat{x}\Psi_{lm}(R,\varphi) \cdot e^{i\beta z} = \tag{10}$$
$$= \hat{x} e^{i\beta z} \begin{cases} F_l(R) \cdot \cos(l\varphi) \\ F_l(R) \cdot \sin(l\varphi) \end{cases}$$

$$F_l(R) = \begin{cases} J_l(uR), & 0 \le R \le 1 \\ K_l(uR), & R \ge 1 \end{cases} \tag{11}$$

$$R = r/a \qquad u = a\sqrt{k^2 n_1^2 - \beta_{lm}^2} \qquad u = a\sqrt{\beta_{lm}^2 - k^2 n_2^2} \tag{12}$$

Where a is the fiber core radius, k is the wave number and β_{lm} is the propagation constant of the LP_{lm} mode. Finally, the coupling coefficient of the j-th outer mode (defined by modal indexes m_j and l_j) can be computed by:

$$c_j = \frac{\sum_k c'_k \dfrac{\iint_{A_\infty} \Psi_{l_k m_k}(R',\varphi') \cdot \Psi_{l_j m_j}(R,\varphi) R dR d\varphi}{\iint_{A_\infty} \left| \Psi_{l_k m_k}(R',\varphi') \right|^2 R dR d\varphi}}{\iint_{A_\infty} \left| \Psi_{l_j m_j}(R,\varphi) \right|^2 R dR d\varphi} \tag{13}$$

The lateral offset is defined by the radial offset (r_0, or equally expressed normalized by the fiber core radius $R_0 = r_0/a$), the angular offset (φ_0), and angular rotation (φ_i) as in Fig. 3. If we consider the axes of the outer fiber as the reference, the coupling coefficient becomes totally characterized by:

$$c_j = \frac{\sum_k c'_k \dfrac{\iint_{A_\infty} \Psi_{l_k m_k}(R',\varphi') \cdot \exp(-ikn_1 a\varphi_i) \cdot \Psi_{l_j m_j}(R,\varphi) R dR d\varphi}{\iint_{A_\infty} \left| \Psi_{l_k m_k}(R',\varphi') \right|^2 R dR d\varphi}}{\iint_{A_\infty} \left| \Psi_{l_j m_j}(R,\varphi) \right|^2 R dR d\varphi} \tag{14}$$

$$R' = \sqrt{R^2 + R_0^2 - 2R^2 R_0^2 \cos(\varphi - \varphi_0)} \tag{15}$$

$$\varphi' = \tan^{-1}\left(\frac{R\sin(\varphi) - R_0 \sin(\varphi_0)}{R\cos(\varphi) - R_0 \cos(\varphi_0)} \right) \tag{16}$$

REFERENCES

[1] IEEE Standard for Ethernet, IEEE Standard 802.3, 2015.

[2] Characteristics of a single-mode optical fibre and cable, Recommendation ITU-T G.652, 2009.

[3] Z. Tian, C. Chen, and D. Plant, "850-nm VCSEL transmission over standard SMF using fiber mode filter," *IEEE Photon. Technol. Lett*., vol. 24, no. 5, pp. 368-370, Mar. 2012.

[4] K. Balemarthy, A. Polley, and S. E. Ralph, "Electronic Equalization of Multikilometer 10-Gb/s Multimode Fiber Links: Mode-Coupling Effects," *J. Lightw. Technol.*, vol. 24, no. 12, pp. 4885-4894, Dec. 2006.

[5] S. Ariyavisitakul, "A decision-feedback equalizer with selective time-reversal structure", *IEEE J. Sel. Areas Commun.*, vol. 10, no. 3, Apr. 1992.

[6] J. Balakrishnan, and C. R. Johnson, "Time-reversal diversity in DFE equalization," in *Proc. Allerton Conf. Commun., Control, and Computing*, Monticello (VA), 2000.

[7] K. Nakajima, J. Zhou, K. Tajima, K. Kurokawa, C. Fukai, and I. Sankawa, "Ultrawide-Band Single-Mode Transmission Performance in a Low-Loss Photonic Crystal Fiber," *J. Lightw. Technol.*, vol. 23, no. 1, pp. 7-12, Jan. 2005.

[8] R. Ries, "Signal transmission with optical carriers in multimode range of single-mode fibres," *Electronics Letters*, vol. 23, pp. 71-72, Jan. 1987.

[9] P. Schnitzer, R. Jager, C. Jung, R. Michalzik, D. Wiedenmann, F. Mederer, and K. J. Ebeling, "Biased and Bias-Free Multi-Gb/s Data Links Using GaAs VCSEL's and 1300-nm Single-Mode Fiber," *IEEE Photon. Technol. Lett*., vol. 10, no. 12, pp. 1781-1783, Dec. 1998.

[10] D. Vez, S.G. Hunziker, R. Kohler, P. Royo, M. Moser, and W. Bächtold, "850 nm vertical-cavity laser pigtailed to standard singlemode fibre for radio over fibre transmission," *Electronics Letters*, vol. 40, no19, pp. 1210-1211, Sep. 2004.

[11] T. Niiho, K. Masuda, H. Sasai, and M. Fuse, "Proposal of RoF transmission system using 850 nm VCSEL and 1.3 gm SMF with low-frequency superposition technique," in *Conf. on Optical Fiber Communication and the Nat. Fiber Optic Engineers Conf. (OFC/NFOEC)*, 2006.

[12] S. Moon, and D. Y. Kim, "Effective single-mode transmission at wavelengths shorter than the cutoff wavelength of an optical fiber," *IEEE Photon. Technol. Lett*., vol. 17, no 12, pp. 2604-2606, Dec 2005.

[13] I. Papakonstantinou, S. Papadopoulos, C. Soos, J. Troska, F. Vasey, and P Vichoudis, "Modal Dispersion Mitigation in Standard Single-Mode Fibers at 850 nm with Fiber Mode Filters", *IEEE Photon. Technol. Lett.*, vol. 22, no 20, pp. 1476-1478, Oct. 2010.

[14] D. Đonlagic, "In-Line Higher Order Mode Filters Based on Long Highly Uniform Fiber Tapers," *J. Lightw. Technol.*, vol. 24, no 9, pp. 3532-3539, Sept. 2006.

[15] J. Nanni, G. Tartarini, S. Rusticelli, F. Perini, C. Viana, J. Polleux, C. Algani, "Modal noise in 850nm VCSEL-based radio over fiber systems for manifold applications," in *Fotonica AEIT Italian Conference on Photonics Technologies,* Italy, 2015

[16] M. Stach, F.I. Pomarico, D. Wiedenmann, R. Michalzik, "High-Performance Low-Cost Optical Link at 850 nm with Optimized Standard Singlemode Fiber and High-Speed Singlemode VCSEL," in *European Conf. and Exhibition on Optical Communications (ECOC)*, pp. 712–713, 2004.

[17] K. Hoa, J. M. Kahn, "Chapter 11. Mode Coupling and its Impact on Spatially Multiplexed Systems," in *Optical Fiber Telecommunications Volume VIB: Systems and Networks*, 6th ed., Ed. Academic Press: Elsevier, 2013, pp. 491–568.

[18] P. Pepeljugoski, M. J. Hackert, J. S. Abbott, S. E. Swanson, S. E. Golowich, A. J. Ritger, P. Kolesar, Y. C. Chen, and P. Pleunis, "Development of System Specification for Laser-Optimized 50-µm Multimode Fiber for Multigigabit Short-Wavelength LANs," *J. Lightw. Technol.*, vol. 21, no 5, pp. 1256-1275, May 2003.

[19] A. W. Snyder, J. D. Love, "Chapter 20 – Illumination, tilts and offsets," in *Optical Waveguide Theory*, 1st ed., Ed. Chapman and Hall, 1983, pp. 420–441.

[20] K. Petermann, "Nonlinear Distortions and Noise in Optical Communication Systems due to Fiber Connectors," *IEEE J. Quantum Electron.*, vol. QE-16, no 7, pp. 761-770, Jul. 1980.t

[21] Y. Jung, G. Brambilla, and D. J. Richardson, "Broadband single-mode operation of standard optical fibers by using a sub-wavelength optical wire filter," *Optics Express*, vol. 16, no. 19, pp. 14661-14667, 2008.

[22] J. G. Proakis, "Chapter 10. Communications through Band-Limited Linear filter Channels," in *Digital Communications*, Ed. McGraw-Hill Higher Education, 2000, pp. 583-635.

[23] N. Al-Dhahir, and J. M. Cioffi, "MMSE Decision-Feedback Equalizers: Finite-Length Results," *IEEE Trans. Inf. Theory*, vol. 41, no. 4, pp 961-975, Jul. 1995.

[24] M. C. Jeruchim, P. Balaban y K. S. Shanmugan, "Chapter 7. Monte Carlo Simulation and Generation of Random Numbers", in *Simulation of Communication Systems. Modeling, Methodology, and Techniques*, Kluwer Academic Publishers, 2002, pp. 371-406.

[25] N. L. Swenson, P. Voois, T. Lindsay, and S. Zeng, "Standards Compliance Testing of Optical Transmitters", in *Conf. on Optical Fiber Communication and the Nat. Fiber Optic Engineers Conf. (OFC/NFOEC)*, Anaheim (CA), USA, 2007.

[26] K. Balemarthy, and S. E. Ralph, "Bidirectional DFEs for 10Gb/s Ethernet over Multimode Fiber Links: Complexity Reduction and Reach Extension", in *Conf. on Optical Fiber Communication and the Nat. Fiber Optic Engineers Conf. (OFC/NFOEC)*, Anaheim (CA), USA, 2007.

[27] R. E. Epworth, "Modal noise-causes and cures," *Laser Focus*, pp. 109-115, 1981.